Kinetic Studies of Reductive Deposition of Copper(II) Ions Photoassisted by Titanium Dioxide

Suzuko Yamazaki* and Shiho Iwai

Department of Chemistry, Faculty of Science, Yamaguchi University, Yamaguchi 753-8512, Japan

Jun Yano

Department of Engineering, University of East Asia, Shimonoseki 751-8503, Japan

Hitoshi Taniguchi

Department of Veterinary Radiology, Faculty of Agriculture, Yamaguchi University, Yamaguchi 753-8515, Japan

Received: July 11, 2001; In Final Form: October 4, 2001

Photoreduction of copper(II) ions onTiO_2 was studied in the presence of sacrificial donors such as HCOONa, $Na_2C_2O_4$, and Na_2H_2edta. Formate was the best donor with respect to the reduction rate but an induction period was observed. The induction period increased with an increase in the Cu(II) concentration or with a decrease in the TiO_2 weight in suspension. The presence of sulfates, phosphates, and chlorides increased the induction period. The ESR measurements indicate that the Cu(II) ions exist as $[Cu(H_2O)_6]^{2+}$ in the formate system while as $[Cu(C_2O_4)_2]^{2-}$ in the oxalate system. The differences in the reduction rates of Cu(II) between the formate and the oxalate system were explained in terms of electrostatic interaction between the Cu(II) complex and the TiO_2 surface and a negative shift in the reduction potential by coordination with oxalate. The following rate law was obtained by kinetic analysis: rate $= \{k_1' K_s N_s [Cu^{II}L] I_a \Phi / (1 + \alpha K_s [Cu^{II}L])\} \times \{K[\text{Donor}]/(1 + K[\text{Donor}])\}$.

Introduction

Much attention has been focused on the photocatalytic degradation of organic pollutants mediated by TiO_2 particles in aqueous suspensions. A lot of works have demonstrated that this method is an effective approach toward the degradation or mineralization of a wide variety of harmful/toxic organic pollutants in wastewaters. However, from a practical viewpoint, the TiO_2 suspension is not appropriate because it requires separation steps to remove the catalyst from the treated water. The fixation of the TiO_2 photocatalyst has been investigated for a coating process using sol−gel technique on substrates such as SiO_2,[1] zeolite,[2] and magnetite.[3] The properties of the TiO_2 films fixed on the substrates depend on the properties of the colloids used to fabricate them.[4] Matsumoto et al. described a new method based on an electrochemical technique to fix a TiO_2 film onto alumite.[5] Remillard et al. prepared amorphous and anatase TiO_2 films with a variety of microstructures by sputtering and pyrolytic deposition and assessed the performance of these films by measuring photooxidation rates of stearic acid on them.[6] Pilkenton et al. have reported the photocatalytic oxidation of ethanol on TiO_2-coated optical microfiber which was prepared by dipping in a TiO_2 dispersion and subsequent heating treatment.[7]

On the other hand, much progress has not been made concerning the kinetics and reaction mechanism. When photons with energies greater than the TiO_2 band gap are absorbed, electron−hole pairs are created, which can migrate to the titania surface where they either recombine or participate in redox reactions with adsorbed species. It is generally believed that the holes oxidize water to hydroxyl radicals and the electrons reduce oxygen to superoxide. These radicals subsequently initiate a chain of reactions that oxidize organic species to completion. Details of further reaction mechanism have remained unclear. There are many papers in which reaction rates were treated empirically to present the same saturation-type kinetic behavior as portrayed by the Langmuir−Hinshelwood rate law.[8] Most of them were obtained on the basis of the rates for photooxidation of organic compounds while there are few papers describing kinetics and rate laws with respect to reduction rates with photogenerated electrons.

It is well-known that metal ions with a standard redox potential more positive to the conduction band of TiO_2 are photoreduced to deposit on titania surface. Tennakone and Wijayantha employed the photoreduction process to extract heavy metals such as Pb and Hg from an aqueous solution.[9] Foster et al. studied reversible photoreductive deposition and oxidative dissolution of copper(II) in TiO_2 suspension.[10] In this paper, we describe the kinetics of the photoreduction of copper(II) ions in order to clarify the reaction mechanism.

Experimental Section

Materials. Degussa P-25 TiO_2 was obtained from Japan Aerosil. The specific surface area was 50 $m^2\ g^{-1}$ and the composition was about 70% anatase and 30% rutile. Other reagents were of the guaranteed reagent grade and used without further purification. Laboratory grade water was prepared with a Milli-Q water system.

Photoreactors. Two types of photoreactors were employed. A batch photoreactor consisted of a 500 mL Pyrex reservoir surrounded by four 4 W fluorescent black light bulbs (Matsushita, FL 4BL-B) which were located in a radial manner at the same interval at the distance of 8 cm from the center of the vessel.

* Author to whom correspondence should be addressed. Telephone & Fax: 81-83-933-5763. E-mail: yamazaki@po.cc.yamaguchi-u.ac.jp.

10.1021/jp012664g CCC: $20.00
Published on Web 11/22/2001

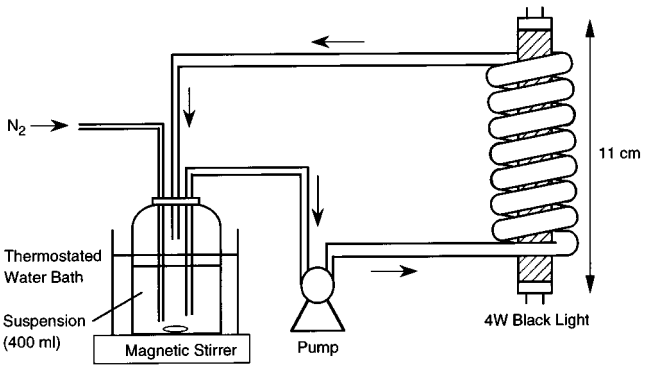

Figure 1. Schematic representation of circulation system.

Figure 1 shows a circulation system consisting of a spiral Pyrex tubing (inner diameter: 7 mm; outer diameter: 9 mm; volume: 30.8 mL). A 4 W fluorescence black light bulb was located at a center of the annulus of the tubing. Two bent Pyrex tubings connected with flexible Tygon tubing through a peristaltic pump were used for recirculating 400 mL of the TiO_2 aqueous suspension containing Cu^{2+} ions in a reservoir which was immersed in a thermostated water bath equipped with a magnetic stirrer (Nissin Thermomeca NT-505D). The volume of the passage which connected the spiral photoreactor with the reservoir was ca. 80 mL. The Tygon tubings were as short as possible and changed with new ones every experiment because of adsorption of TiO_2. The photon flux of the photoreactor was determined by potassium tris(oxalato)ferrate(III) chemical actinometry. The photon flux was estimated to be 3.00×10^{-6} einstein s^{-1} at the wavelength shorter than 400 nm.

Procedures. In both photoreactors, nitrogen was purged through the TiO_2 suspension for 30 min before irradiation. The suspension was purged with nitrogen and vigorously stirred throughout the experiments. Before and after the irradiation, 5 mL samples were withdrawn from the reservoir at appropriate times, immediately transferred into centrifuge tubings under nitrogen atmosphere, and centrifuged at 2000 rpm for 5 min. The concentration of Cu^{2+} in the supernatant liquid was determined by colorimetry (Shimadzu UV-1600) with sodium diethyldithiocarbamate or by spectrometry with inductively coupled plasma (Varian, ICP-AES Liberty Series II). The total volumes withdrawn were limited to be less than 10% of the initial volume of the reaction solution, since a portion of the TiO_2 powders in the reservoir was removed together with the sample solutions.

Spin-Trapping Method. The ESR spin-trapping technique was adopted to identify radicals produced by the irradiation of the TiO_2 suspension. 5,5-Dimethyl-1-pyrroline-*N*-oxide (DMPO) was employed as a diamagnetic radical scavenger. Aqueous suspensions of 1 mL containing 0.2 wt % TiO_2 and 37.5 μL DMPO in the presence or absence of 0.1 mol dm^{-3} HCOONa were irradiated for 20 min and the sample was taken with capillary (hematocrit capillary tubings, Doramond). The ESR spectra were recorded using a JEOL JES-FE1X spectrometer, operating at the X band.

Results and Discussion

A typical variation in the Cu^{2+} concentration in a batch photoreactor was depicted in Figure 2. When an aqueous TiO_2 suspension (0.2 wt %) containing 50 ppm Cu^{2+} (7.9×10^{-4} mol dm^{-3} $CuSO_4$) and 0.1 mol dm^{-3} sodium formate was illuminated under nitrogen atmosphere, the concentration of Cu^{2+} decreased due to reductive deposition on the TiO_2 surface. This process turned the color of TiO_2 to purple. Then, when

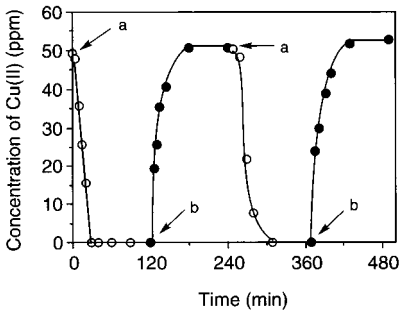

Figure 2. Time course of the Cu(II) concentration when the light was turned on under N_2 purge (a) and turned off under O_2 purge (b). Conditions: 0.1 mol dm^{-3} HCOONa, pH 3.6, 30 °C, 0.2 wt % TiO_2, four lamps were irradiated.

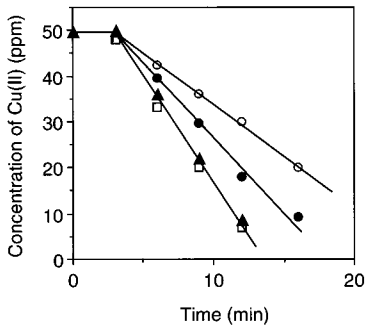

Figure 3. Effect of flow rate. Conditions: 7.9×10^{-4} mol dm^{-3} $CuSO_4$, 0.1 mol dm^{-3} HCOONa, pH 3.6, $\mu = 0.1$ mol dm^{-3}, 30 °C, 0.2 wt % TiO_2. Flow rate was 43 (○), 214 (●),429 (□), and 600 mL min^{-1} (▲).

the suspension was purged with oxygen without irradiation, TiO_2 returned to white and the Cu^{2+} concentration increased to the initial value. The same behavior was observed by repeating the experiment. In this paper, we focus on the reaction rate of the decrease in the Cu^{2+} concentration, which was observed with illumination under a nitrogen atmosphere.

To enhance the rate of reduction of metal ions, it is necessary to use hole-consuming sacrificial agents to avoid the recombination process of holes with electrons. Foster et al. employed formate as a sacrificial donor for recovering copper from wastewaters after electroless copper plating, in which formate was formed by oxidation of formaldehyde.[11] Therefore, first we describe the kinetic results with formate. The kinetic data were obtained using the circulation system as shown in Figure 1, where the reaction temperature was maintained at a constant during the experiments.

A. HCOONa as a Sacrificial Donor. *Effect of Flow Rate.* Reaction rates were measured at various flow rates for circulation of the suspension. Figure 3 indicates that after an induction period of ca. 3.3 min, the Cu^{2+} concentration decreased linearly with irradiation time. The slope of this decrease, i.e., the rates of reduction of Cu^{2+}, increased with increase in flow rate and approached a constant value at flow rates faster than 429 mL min^{-1}. It is noted that the induction period was not dependent on the flow rate. Thereafter, all the experiments were performed at the flow rate above 429 mL min^{-1}.

Effect of Anions and Ionic Strength. When ionic strength (μ) of the reaction solution was adjusted with the addition of $NaNO_3$ or $NaClO_4$, neither slope nor induction period was influenced: the slope was 4.54 ± 0.18 ppm min^{-1} and the induction period was 2.18 ± 0.22 min as listed in Table 1. This finding suggests that the reduction rates for Cu^{2+} was not dependent on ionic strength. However, in the presence of $H_2PO_4^-$ or SO_4^{2-}, the

TABLE 1: Effect of Anions to Adjust Ionic Strength[a]

μ (mol dm^{-3})	additives	slope (ppm min^{-1})	induction period (min)
0.1	none	4.63	1.7
0.3	$NaNO_3$	4.61	2.4
0.5	$NaNO_3$	4.83	2.2
0.3	$NaClO_4$	4.33	2.1
0.5	$NaClO_4$	4.28	2.5
0.3	NaH_2PO_4	0.86	16.3
0.2	NaCl	8.78	5.0
0.3	NaCl	7.07	4.8
0.5	NaCl	6.35	5.9
0.3	Na_2SO_4	3.04	4.7
0.5	Na_2SO_4	1.21	8.6

[a] Conditions: 7.9×10^{-4} mol dm^{-3} $Cu(NO_3)_2$, 0.1 mol dm^{-3} HCOONa, 0.2 wt % TiO_2, pH 3.6, 30 °C.

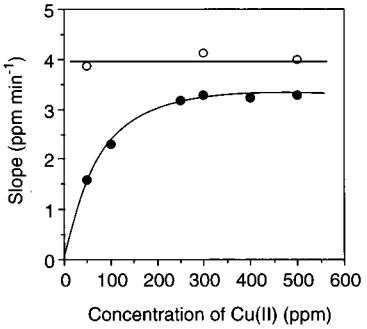

Figure 4. Dependence of slopes on Cu(II) concentrations in the presence of 0.1 mol dm^{-3} HCOONa (○) or $Na_2C_2O_4$ (●). Conditions: pH 3.6, μ = 0.3 mol dm^{-3}, 30 °C, 0.2 wt % TiO_2.

induction periods increased and the slopes decreased. This tendency was obvious with an increase in the SO_4^{2-} concentration. On the other hand, with the addition of 0.1 mol dm^{-3} Cl^- (μ = 0.2 mol dm^{-3}), both the induction period and slope increased to 5.0 min and 8.78 ppm min^{-1}, respectively. The increase in the Cl^- concentration had little effect on the induction period but decreased the slope to 6.35 ppm min^{-1} with 0.4 mol dm^{-3} NaCl (μ = 0.5 mol dm^{-3}).

Abdullah et al. investigated effects of inorganic anions on rates of photocatalytic oxidation of organic compounds and reported that perchlorates and nitrates have little effect while chloride, sulfates, and phosphates reduced the oxidation rates.[12] The latter three anions adsorbed on the TiO_2 and competed with the adsorption of organic compounds. Therefore, the increase in the induction periods in our system is ascribed to the adsorption of these anions, which decreased the number of adsorption sites available to reduction of Cu^{2+}. We observed the reduction rates for Cu^{2+} were accelerated with the addition of Cl^-. This may come from the role of Cl^- bridging between Cu^{2+} and Ti, which promotes inner-sphere electron transfer. Although the reason the reaction occurred suddenly after an induction period was not clear, hereafter the ionic strength was adjusted with $NaNO_3$ and the Cu^{2+} aqueous solutions were prepared with $Cu(NO_3)_2$.

Effect of Cu(II) Concentration. The rates of reduction were independent of initial concentrations of Cu^{2+} as shown in Figure 4 while the induction periods increased with an increase in the Cu^{2+} concentration: 2.4, 4.7, and 5.1 min at the Cu^{2+} concentrations of 50, 300, and 500 ppm, respectively.

Effect of HCOONa Concentration. The dependence of the rates of reduction on the concentration of HCOONa were examined over the range of 0.001−0.2 mol dm^{-3}. The rates increased with the HCOONa concentration and reached a constant value of 3.97 ± 0.04 ppm min^{-1} as Figure 5

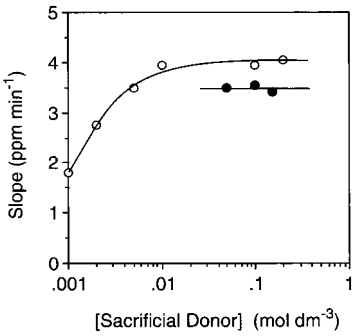

Figure 5. Effect of concentrations of HCOONa (○) or $Na_2C_2O_4$ (●). Conditions: pH 3.6, 30 °C, 0.2 wt % TiO_2. Concentration of Cu(II) and ionic strength were 50 ppm and 0.5 mol dm^{-3} for HCOONa or 500 ppm and 0.3 mol dm^{-3} for $Na_2C_2O_4$.

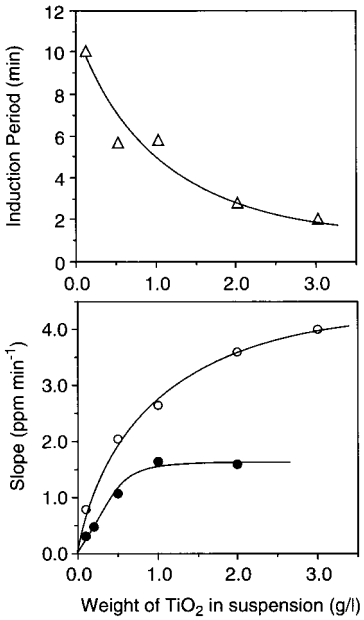

Figure 6. Effect of TiO_2 amounts on induction periods and slopes in the presence of 0.1 mol dm^{-3} HCOONa (△, ○) at μ = 0.1 mol dm^{-3} or $Na_2C_2O_4$ (●) at μ = 0.3 mol dm^{-3}. Conditions: 50 ppm Cu(II), pH 3.6, 30 °C.

represented. On the contrary, as the concentration increased, the induction period decreased: 6.0 min at 0.001 mol dm^{-3}; 3.5 min at 0.002 mol dm^{-3}; and 2.31 ± 0.41 min above 0.005 mol dm^{-3}.

Effect of TiO_2 Amount. The effect of the amount of dispersed TiO_2 on the induction periods and the reduction rates were presented in Figure 6. The induction period of 10.2 min at 0.1 g L^{-1} TiO_2 decreased to 2.2 min at 3.0 g L^{-1}. On the other hand, the reduction rates of 0.79 ppm min^{-1} at 0.1 g L^{-1} increased with the TiO_2 amount to 3.99 ppm min^{-1} at 3.0 g L^{-1}.

Effect of Reaction Temperature. The induction period was not dependent on reaction temperature over the range of 30.0−50.5 °C. However, the reduction rates increased gradually with temperature: 4.52, 4.90, and 6.20 ppm min^{-1} at 30.0, 40.0, and 50.5 °C.

Spin Trapping Method for Determining the Radical Intermediates. Convincing evidence for the generation of the OH radical upon irradiation of aqueous solutions of TiO_2 has been obtained from use of spin traps capable of scavenging the OH radicals and producing a characteristic nitroxide which can be detected by ESR.[13] Table 2 lists the observed ESR parameters for spin adducts with DMPO with or without HCOONa. In the

TABLE 2: ESR Parameters for Spin Adducts with DMPO

sample	a^N(G)	a^H(G)
(1) TiO_2 aqueous suspension (UV)	15.0	15.0
(2) HCOONa + (1) (UV)	16.0	19.0

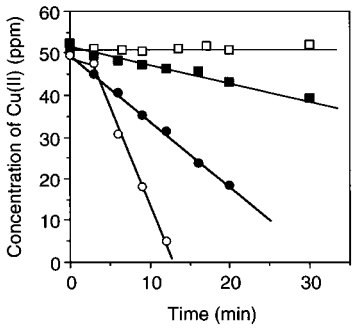

Figure 7. Effect of sacrificial donors of 0.1 mol dm^{-3} HCOONa (○), $Na_2C_2O_4$ (●), Na_2H_2edta (■), or CH_3COONa (□). Conditions: pH 3.6, μ = 0.3 mol dm^{-3}, 30 °C, 0.2 wt % TiO_2.

absence of HCOONa, hyperfine coupling constants were analyzed to be 15.0 G for both a^N and a^H, which are coincident to the reported values for DMPO−OH adducts (14.90 G).[14] On the other hand, in the presence of HCOONa, the a^N and a^H values were estimated to be 16.0 and 19.0 G, respectively. Hyperfine coupling constants for DMPO−CO_2 adducts were reported to be 15.79 G for a^N and 18.97 G for a^H, respectively.[14] Therefore, addition of HCOONa produced a CO_2^- radical under illumination, which was caused by trapping photogenerated holes with formate.

$$TiO_2 + h\nu \rightarrow h^+ + e^- \quad (1)$$

$$h^+ + e^- \rightarrow \text{recombination} \quad (2)$$

$$h^+ + HCOO^- \rightarrow H^+ + CO_2^- \quad (3)$$

$$h^+ + CO_2^- \rightarrow CO_2 \quad (4)$$

B. Effect of Sacrificial Donor. We examined the effect of sacrificial donors by using 0.1 mol dm^{-3} of $Na_2C_2O_4$, Na_2H_2-edta (edta: ethylenediaminetetraacetate) or CH_3COONa instead of HCOONa. As shown in Figure 7, no appreciable change in the Cu(II) concentration was observed with CH_3COONa. It is noted that an induction period was observed only with HCOONa. The reduction rates of Cu(II), i.e., the slopes, were estimated to be 4.69, 1.60, and 0.40 ppm min^{-1} for HCOONa, $Na_2C_2O_4$, and Na_2H_2edta, respectively, indicating that HCOONa was the best donor for the Cu(II) photodeposition. On the other hand, from the viewpoint of the standard redox potentials, the reactivity with holes decreases as the following order: Na_2H_2-edta > $Na_2C_2O_4$ > HCOONa. These findings suggest that these donors do not act only for consuming the photogenerated holes. The oxidation process of Na_2H_2edta was very complicated while both HCOONa and $Na_2C_2O_4$ were simply oxidized to CO_2. Thus, the kinetic data for HCOONa and $Na_2C_2O_4$ were compared in details.

Effect of Reactants' Concentrations in the Case of $Na_2C_2O_4$ as a Sacrificial Donor. Dependence of the reduction rates on the initial concentration of Cu(II) was presented in Figure 4. The slope increased with an increase in the Cu(II) concentration and reached a limiting value of 3.26 ± 0.02 ppm min^{-1} at concentration more than 300 ppm. It is worthy to note that no such dependence was observed for HCOONa and the slopes

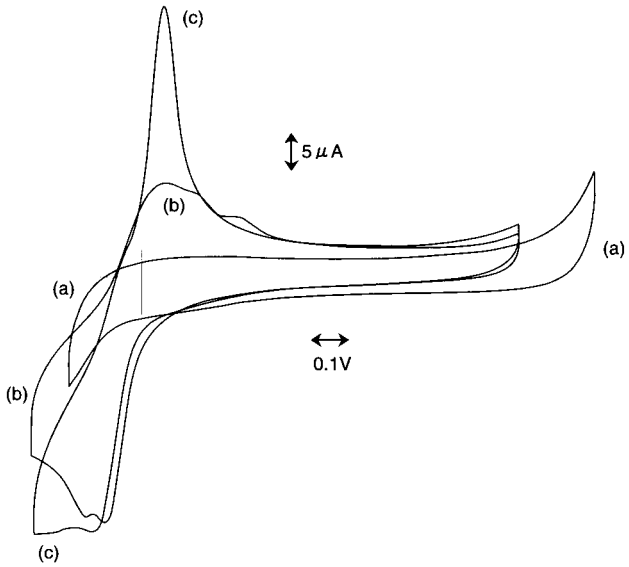

Figure 8. Cyclic voltammograms in 0.3 mol dm^{-3} $NaNO_3$ solutions at pH 3.6. (a) None, (b) 50 ppm Cu^{2+}, (c) 50 ppm Cu^{2+} and 0.1 mol dm^{-3} HCOONa.

(3.99 ± 0.09 ppm min^{-1}) were larger by a factor of 1.2 than the maximum rate observed with $Na_2C_2O_4$.

The slopes obtained with 500 ppm Cu(II) solutions containing 0.05, 0.1, and 0.15 mol dm^{-3} $Na_2C_2O_4$ were shown in Figure 5. The mean value for the slopes was 3.48 ± 0.05 ppm min^{-1} which was smaller by a factor of 1.1 than the maximum rates observed with HCOONa. If formate and oxalate act as sacrificial donors for consuming the photogenerated holes, the maximum rates should be the same. However, these data suggest that the presence of oxalate retarded the photoreduction of Cu(II). Figure 6 also represented that the slopes increased with the TiO_2 amount and reached a plateau of 1.62 ± 0.02 ppm min^{-1} which was smaller than that with HCOONa.

Cyclic Voltammetry. Cyclic voltammogram using glassy carbon as a working electrode was measured in 50 ppm Cu(II) aqueous solutions in the absence or presence of sacrificial donors. As shown in Figure 8, addition of 0.1 mol dm^{-3} HCOONa did not affect the redox potential of Cu(II) ion, −0.02 V vs SCE, which was calculated from potentials at anodic and cathodic peak currents, although the reason an anodic peak without HCOONa was not as sharp as the cathodic peak was unclear. On the other hand, in the presence of $Na_2C_2O_4$ and Na_2H_2edta, reduction of Cu(II) was not observed in the potential region up to −0.2 V. This finding indicates that it is more difficult to reduce Cu(II) ions in the presence of $Na_2C_2O_4$ and Na_2H_2edta.

ESR Measurements. The ESR measurements were performed at room temperature since they often give us information about microscopic structures around the paramagnetic center. The addition of $Na_2C_2O_4$ to a $Cu(NO_3)_2$ solution gave a spectrum which consisted of four hyperfine lines corresponding to the Cu nuclear spin of 3/2 as shown in Figure 9c. Such hyperfine structures were clearly observed for various Cu^{2+} complexes produced by replacing the coordinated water with nitrogen-containing ligands or various carboxylates.[15] On the other hand, as shown in Figure 9a, the $[Cu(H_2O)_6]^{2+}$ yielded a broad spectrum due to spin-exchange interaction. In Figure 9b, a similar spectrum was obtained with HCOONa, indicating that its addition did not affect the environments around the Cu^{2+} ions. Therefore, the Cu^{2+} exists as $[Cu(H_2O)_6]^{2+}$ in the presence of HCOONa while as $[Cu(C_2O_4)_2]^{2-}$ with $Na_2C_2O_4$. The data

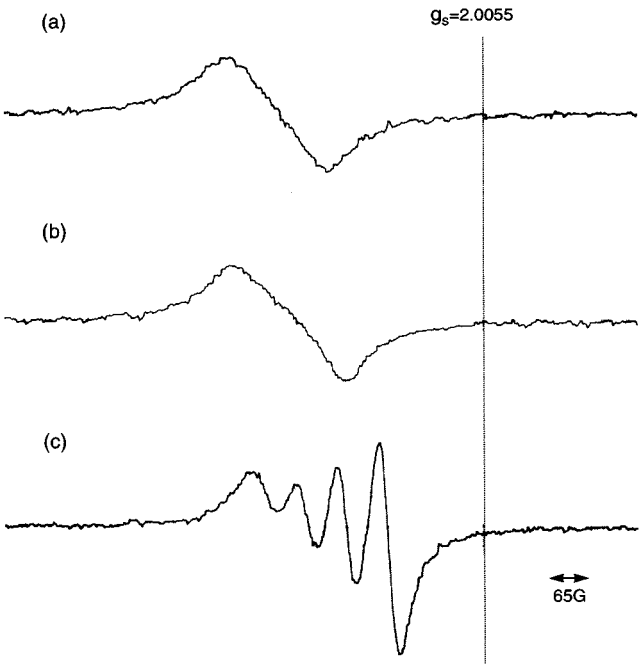

Figure 9. ESR spectra of 500 ppm Cu^{2+} aqueous solutions at pH 3.6. (a) No sacrificial donors, (b) 0.1 mol dm^{-3} HCOONa, (c) 0.1 mol dm^{-3} $Na_2C_2O_4$. The vertical line indicates a line position of Fremy salt (g_s = 2.0055).

obtained by the voltammetry indicate that the coordination with $C_2O_4^{2-}$ or $edta^{4-}$ makes the Cu^{2+} more difficult to be reduced.

C. Mechanistic Aspects. The following reaction mechanism can be postulated to account for the obtained experimental data:

$$(\text{site}) + Cu^{II}L \underset{k_d}{\overset{k_a}{\rightleftharpoons}} Cu^{II}L(\text{ads}) \xrightarrow{k_1} Cu^{I}L(\text{ads}) \xrightarrow{k_2} Cu^{0}L(\text{ads}) \quad (5)$$

where k_a, k_d, k_1, and k_2 represent rate constants for adsorption and desorption of $Cu^{II}L$ and for reduction of $Cu^{II}L$(ads) and $Cu^{I}L$(ads), respectively. The $Cu^{II}L$ corresponds to $[Cu(H_2O)_6]^{2+}$ or $[Cu(C_2O_4)_2]^{2-}$ with the addition of HCOONa or $Na_2C_2O_4$, respectively, and (ads) indicates species adsorbed on TiO_2.

Assuming the steady-state concentrations for $Cu^{II}L$(ads), the following equations are obtained:

$$\text{rate} = -\text{d}[Cu^{II}L]/\text{d}t = k_a S_v [Cu^{II}L] - k_d S^{II} = k_1 S^{II} = k_1 K_s S_v [Cu^{II}L] \quad (6)$$

where S_v and S^{II} mean the number of vacant sites and the sites adsorbed by $Cu^{II}L$, respectively, and K_s denotes $k_a/(k_d + k_1)$. Introducing the total number of the adsorbed sites, N_s, which is the sum of S_v, S^{II}, S^{I}, and S^0 and assuming the steady-state conditions for $Cu^{I}L$(ads), eq 6 is converted to eq 7

$$\text{rate} = k_1 K_s N_s [Cu^{II}L]/(1 + \alpha K_s [Cu^{II}L]) \quad (7)$$

where α presents $(k_1 + k_2)/k_2$ and the value of $(N_s - S^0)$ is assumed to approximately equal N_s. The rate constant k_1 is proportional to the amounts of electrons which have escaped from recombination with holes.

The more holes are consumed by the reaction with sacrificial donors, the more electrons are available for reduction of copper (see eqs 1−4). Thus, the value of k_1 is proportional to $I_a\Phi \cdot \theta_{donor}$ where I_a and Φ indicate, respectively, the intensity of absorbed light and quantum yield for generation of electron/hole pairs which are separated into conduction band electrons and valence band holes. The fractional coverages, θ_{donor}, is a function of concentrations of sacrificial donors according to Langmuir−Hinshelwood kinetic models.[16] Finally, the rate law is expressed as follows:

$$\text{rate} = \{k_1' K_s N_s [Cu^{II}L] I_a \Phi/(1 + \alpha K_s [Cu^{II}L])\} \times \{K[\text{Donor}]/(1 + K[\text{Donor}])\} \quad (8)$$

Here we assume that the oxidation with holes and the reduction with electrons occur on the different surface sites on the catalyst.

The second term in eq 8, the adsorption isotherm expression for the sacrificial donor, is responsible to the effect of concentrations of formate on the reduction rate of copper(II) as in Figure 5. The dependence of the rates on the TiO_2 amount is explained in terms of the absorbed light intensity which is given by eq 9:

$$I_a = I_o \{1 - \exp(-\gamma C)\} \quad (9)$$

where I_o is the intensity of incident light, γ is a constant relating to the length of the light path and absorptivity of TiO_2, and C is the amount of TiO_2. Clearly, more TiO_2 yields more light-absorption and I_a approaches a limiting value where all the incident light is absorbed.

The reaction rate was not dependent on the Cu(II) concentration in the presence of formate as shown in Figure 4. This finding suggests the relation, $1 \ll \alpha K_s [Cu^{II}L]$, in the denominator of the first term in eq 8. Thus, the rate is constant to be $(k_1' N_s I_a \Phi/\alpha)\theta_{donor}$ which can explain the behavior that the Cu(II) concentration decreased linearly with the irradiation time.

According to the manufacturer, the pH of the isoelectric point of Degussa P-25 is 6.6, and thus the TiO_2 has positive charge at pH 3.6 and attracts negatively charged species. Since the Cu(II) ions exist as $[Cu(C_2O_4)_2]^{2-}$ or $[Cu(H_2O)_6]^{2+}$, respectively, in the presence of oxalate or formate, we would expect in the oxalate system that the k_a is higher and k_d is smaller than in the formate system. Besides the cyclic voltammetry measurements suggest that the k_1 value in the oxalate system is smaller than that in the formate system. Therefore, $(K_s)_{oxalate} > (K_s)_{formate}$. On the other hand, the k_2 value in the oxalate system is expected to be much higher than that in the formate system because of a rapid intermolecular electron transfer as shown in eq 10:

$$[Cu^{I}(C_2O_4)_2]^{3-} \rightarrow [Cu^{0}(C_2O_4)]^{2-} + CO_2 + CO_2^{-} \quad (10)$$

Thus, $(\alpha)_{oxalate} \ll (\alpha)_{formate}$. As a result, the relation of $(\alpha K_s)_{oxalate} < (\alpha K_s)_{formate}$ holds and we observed in the oxalate system the region where the rate depended on the Cu(II) concentration. The difference in the maximum rate means $(k_1'/\alpha)_{oxalate} \times \theta_{oxalate} < (k_1'/\alpha)_{formate} \times \theta_{formate}$.

The induction period observed with formate decreased drastically with an increase in the TiO_2 amount and increased with the addition of PO_4^{3-}, SO_4^{2-}, and Cl^- which are adsorbed on the TiO_2 surface. No induction periods were observed in the oxalate system where the $[Cu(C_2O_4)_2]^{2-}$ adsorbed easily on the catalyst. These findings suggest that induction period relates to the number of adsorption sites occupied with Cu(II) species. However, an increase in the Cu(II) concentration increased the induction period. This behavior may indicate the disproportionation between the Cu(I) species adsorbed on adjacent sites.

$$2Cu^{I}L(\text{ads}) \rightarrow Cu^{II}L(\text{ads}) + Cu^{0}L(\text{ads}) \quad (11)$$

Such disproportionation is ruled out in the oxalate system because of $k_1 \ll k_2$.

The induction period might be effected by a trace of oxygen which strongly adsorbed on the catalyst surface and was not removable by nitrogen purging. Further work is necessary to clarify the origin of the induction period.

Conclusion

Formate acts as an effective sacrificial donor for consuming photogenerated holes and facilitates the Cu(II) photodeposition on TiO_2. The Cu(II) ions exist as $[Cu(H_2O)_6]^{2+}$ in the formate system while as $[Cu(C_2O_4)_2]^{2-}$ in the oxalate system. The differences in the reduction rates of Cu(II) between the formate and the oxalate system were explained in terms of electrostatic interaction between the Cu(II) complex and the TiO_2 surface and a negative shift in the reduction potential by coordination with oxalate.

Carboxylic acids such as formate, oxalate, EDTA, salicylic acid, and citric acid have been employed as hole-consuming sacrificial agents in the application of photocatalysts for decontaminating heavy-metal polluted water. This work indicates that we must pay attention to the formation of complexes and select a suitable donor in order not to retard the reduction process.

Degussa P-25 powders are difficult to use for practical purposes because of the necessity of filtration for a recovery of the catalyst. We are now investigating the photodeposition of metal ions on the TiO_2 membrane.

Acknowledgment. This work was partially supported by the UBE Foundation. We thank Prof. Emeritus K. Ishizu for discussion on the ESR data. We also thank the Center of Instrumental Analysis at Yamaguchi University for measurements with ICP.

References and Notes

(1) (a) Kim, W. B.; Choi, S. H.; Lee, J. S. *J. Phys. Chem. B* **2000**, *104*, 8670. (b)Yamashita, H.; Kawasaki, S.; Ichihashi, Y.; Harada, M.; Takeuchi, M.; Anpo, M.; Stewart, G.; Fox, M. A.; Louis, C.; Che, M. *J. Phys. Chem. B* **1998**, *102*, 5870.

(2) Vaisman, E.; Cook, R. L.; Langford, C. H. *J. Phys. Chem. B* **2000**, *104*, 8679.

(3) Beydoun, D.; Amal, R.; Low, G. K.-C.; McEvoy, S. *J. Phys. Chem. B* **2000**, *104*, 4387.

(4) (a) Zaban, A.; Aruna, S. T.; Tirosh, S.; Gregg, B. A.; Mastai, Y. *J. Phys. Chem. B* **2000**, *104*, 4130. (b) Luca, V.; Djajanti, S.; Howe, R. F. *J. Phys. Chem. B* **1998**, *102*, 10650.

(5) Matsumoto, Y.; Ishikawa, Y.; Nishida, M.; Ii, S. *J. Phys. Chem. B* **2000**, *104*, 4204.

(6) Remillard, J. T.; McBride, J. R.; Nietering, K. E.; Drews, A. R.; Zhang, X. *J. Phys. Chem. B* **2000**, *104*, 4440.

(7) Pilkenton, S.; Hwang, S.-J.; Raftery, D. *J. Phys. Chem. B* **1999**, *193*, 11152.

(8) (a)Bahnemann, D.; Cunningham, J.; Fox, M. A.; Pelizzetti, E.; Pichat, P.; Serpone, N. In *Aquatic and Surface Photochemistry*; Helz, R., Zepp, R. G., Crosby, D. G., Eds.; CRC Press: Boca Raton, FL, 1994; p 261. (b) Hoffmann, M. R.; Martin, S. T.; Choi, W.; Bahnemann, D. W. *Chem. Rev.* **1995**, *95*, 69.

(9) Tennakone, K.; Wijayantha, K. G. U. *J. Photochem. Photobiol. A: Chem.* **1998**, *113*, 89.

(10) Foster, N. S.; Noble, R. D.; Koval, C. A. *Environ. Sci. Technol.* **1993**, *27*, 350.

(11) Foster, N. S.; Brown, G. N.; Noble, R. D.; Koval, C. A. In *Photocatalytic Purification and Treatment of Water and Air*; Ollis, D. F., Al-Ekabi, H., Eds.; Elsevier: Amsterdam, 1993; p 365.

(12) Abdullah, M.; Low, G. K.-C.; Matthews, R. W. *J. Phys. Chem.* **1990**, *94*, 6820.

(13) Schwarz, P. F.; Turro, N. J.; Bossmann, S. H.; Braun, A. M.; Wahab, A.-M. A. A.; Durr, H. *J. Phys. Chem. B* **1997**, *101*, 7127.

(14) (a) Kirino, Y.; Ohkuma, T.; Kwan, T. *Chem. Pharm. Bull.* **1981**, *29*, 29. (b) Buettner, G. R. *Free Rad. Biol. Med.* **1987**, *3*, 259.

(15) (a) Fujisawa, K.; Kobayashi, T.; Fujita, K.; Kitajima, N.; Morooka, Y.; Miyashita, Y.; Yamada, Y.; Okamoto, K. *Bull. Chem. Soc. Jpn.* **2000**, *73*, 1797. (b) Yamauchi, J.; Yano, S. *Makromol. Chem.* **1988**, *189*, 939. (c) Wilson, R.; Kivelson, D. *J. Chem. Phys.* **1966**, *44*, 4445.

(16) Hill, C. G., Jr. *Introduction to Chemical Engineering Kinetics and Reactor Design*; John Wiley & Sons: New York, 1977.